

# QSAR studies and pharmacophore identification for arylsubstituted cycloalkenecarboxylic acid methyl esters with affinity for the human dopamine transporter

Helena S. Christensen,<sup>a</sup> Søren V. Boye,<sup>a</sup> Jacob Thinggaard,<sup>a</sup> Steffen Sinning,<sup>b</sup>  
Ove Wiborg,<sup>b</sup> Birgit Schiøtt<sup>a,\*</sup> and Mikael Bols<sup>a,\*</sup>

<sup>a</sup>Department of Chemistry, University of Aarhus, Langelandsgade 140, DK-8000 Aarhus C, Denmark

<sup>b</sup>Department of Biological Psychiatry, Psychiatric, University Hospital, Skovagervej 2, DK-8240 Risskov, Denmark

Received 18 September 2006; revised 25 February 2007; accepted 4 May 2007

Available online 10 May 2007

**Abstract**—Data from a series of 29 monoamine transport inhibitors were used to generate 2D and 3D QSAR models for their binding affinity to the human dopamine transporter (hDAT). Among the inhibitors were many non-nitrogen containing compounds. The 2D QSAR analysis resulted in the equation  $-\log K_i = 4.00 - 3.93E_{LUMO} - 0.67E_{HOMO} - 3.24\sigma_p$ , which predicted the importance of electron withdrawing groups in the aromatic moiety. However, the model failed to predict the observed poor binding of nitro-substituted compounds. In contrast, a derived 3D QSAR model was capable of predicting these more correctly.

© 2007 Elsevier Ltd. All rights reserved.

## 1. Introduction

Cocaine (**1**) is one of the most addictive substances known, and currently no efficient treatment is available.<sup>1</sup> It exerts its stimulating and reinforcing effect by inhibiting the reuptake of the three major monoamines, dopamine (DA), serotonin (SER) and norepinephrine (NE), into the presynaptic neuron by blocking their respective transporters [dopamine transporter (DAT), serotonin transporter (SERT) and norepinephrine transporter (NET)]. This blockade results in an elevated synaptic content of monoamines and consequently an enhanced response to the incoming signal. It has for some time

been accepted as the current view of the ‘dopamine hypothesis’ that it is the increased amount of DA and its subsequent action at one or more of the D<sub>1</sub>–D<sub>5</sub> DA receptors, and not a directly mediated message by the binding of cocaine itself, that at large is responsible for the behaviours associated with cocaine addiction.<sup>2,3</sup> As a consequence of this assumption, the DAT has become the major target in several studies in the search of a treatment of cocaine addiction<sup>4</sup> even though cocaine’s affinities for the three major monoamine transporters are roughly similar.<sup>2,5</sup> Recent studies also imply that the biochemistry may not be this simple, since cocaine seems to interact with the metabotropic glutamate receptor (mGluR) as well.<sup>6</sup> However, most studies conducted in this area are focused on the discovery of selective DAT inhibitors that are either cocaine antagonists or partial agonists. The latter operate as competing antagonists in the presence of a full antagonist (cocaine), and can thus be utilized for potential treatment of cocaine abuse provided the addictive properties of the substitute are smaller.

Over the past two decades, there have been an increasing number of studies in the literature of the chemical and pharmacological profiles of several classes of DAT inhibitors, **Figure 1**, including tropanes (mainly of the WIN based-analogues (**2**)),<sup>7,8</sup> benztropine-based

*Abbreviations:* hDAT, human dopamine transporter; hSERT, human serotonin transporter; hNET, human norepinephrine transporter; DA, dopamine; SER, serotonin; NE, norepinephrine; QSAR, quantitative structure–activity relationship; 2D, 2 dimensional; 3D, 3 dimensional; CoMFA, Comparative Molecular Field Analysis; NBS, *N*-bromosuccinimide; TFA, trifluoroacetic acid; Tf<sub>2</sub>O, triflic anhydride; TS, training set; TES, test set; G/PLS, Genetic Partial Least Squares; PLS, Partial Least squares; GFA, Genetic Function Approximation; PRE-SS, predictive residual sum of squares; RMS, root mean square; DCM, dichloromethane.

*Keywords:* Monoamine transporters; QSAR; Inhibitors.

\* Corresponding authors. Tel.: +45 8942 3963 (M.B.); e-mail addresses: [birgit@chem.au.dk](mailto:birgit@chem.au.dk); [mb@chem.au.dk](mailto:mb@chem.au.dk)

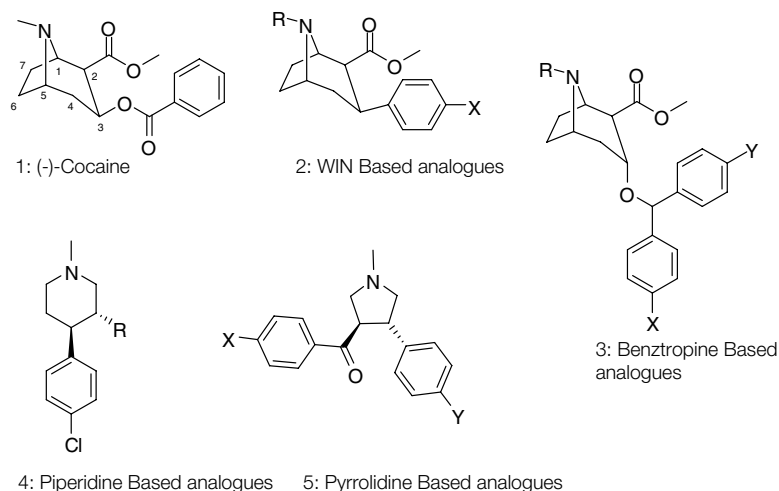


**Figure 1.** Structures of cocaine and selected analogues.

analogues (**3**),<sup>5,9</sup> as well as piperidine-based analogues (**4**).<sup>10,11</sup> Lately, a new type of pyrrolidine-based analogues (**5**)<sup>12,13</sup> has gained interest in the continuing search for potent DAT inhibitors. Many of these studies have expanded from including only synthesis, structure–activity relationships (SAR) and pharmacology to furthermore include, for example, a Comparative Molecular Field Analysis (CoMFA)<sup>14</sup> of the compounds.<sup>15–18</sup> CoMFA-studies are conducted by using activity data to gain valuable knowledge of structural features required for the set of compounds studied to achieve optimal binding to the DAT, that is, generation of a pharmacophore model for optimal binding in the ligand binding-site of the DAT. The studies resulted in predictive models for the behaviour of benztropine analogues **3** and piperidine analogues **4** that among others came to the conclusion that small halogens (–Cl, –F) in *meta*–

*para* positions on the phenyl-moiety were well tolerated. To the best of our knowledge, no one has yet conducted any CoMFA or other 3D QSAR studies on aryl-substituted cycloalkenecarboxylic acid methyl esters of the type that can be seen in Figure 4. These compounds are interesting to study because they, despite losing the important nitrogen atom in most compounds, possess considerable binding affinity. This raises the question whether the compounds still bind in the same mode as cocaine and phenyltropanes. Therefore, we set out to fill this gap by exploiting first 2D QSAR (Cerius2<sup>19</sup>) and subsequently the 3D methodology implemented in Catalyst<sup>20</sup> in order to gain more knowledge of this specific group of DAT inhibitors with respect to extracting the most important structural and electronic properties required to achieve optimal binding to hDAT.

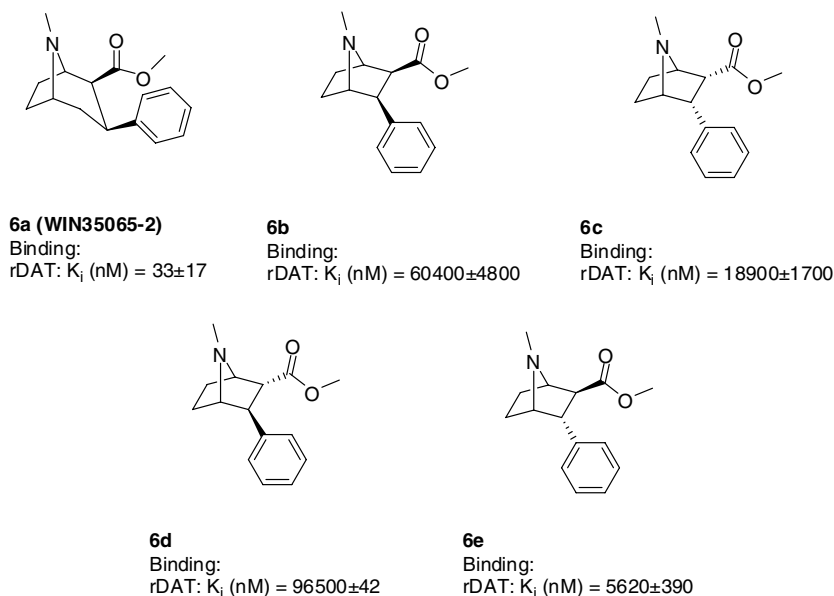
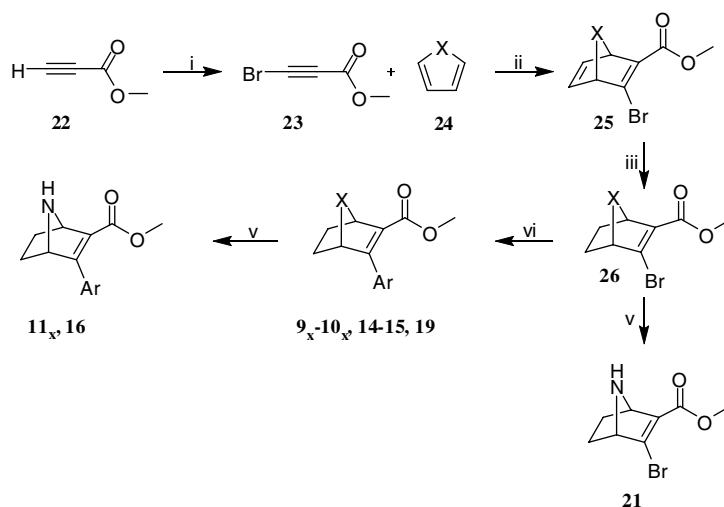


**Figure 2.** Ring-contracted analogues of the phenyl tropane WIN35065-2.

Structural modification in several, different positions of the phenyl tropane has previously been addressed (2, Fig. 1). However, simplification of the phenyl tropane skeleton has not received much attention.

One such work has been carried out by the Trudell group.<sup>21</sup> They synthesized the ring-contracted analogues (6b–e, Fig. 2) of the phenyl tropane WIN35065-2 (6a) and investigated their binding to the DAT. While the synthesis of the 2:2:1-azabicyclic system was short and elegant, mainly following the transformation 25 → 26 → 11 (Scheme 1), reduction of the double bond and separation of the diastereoisomers 6b–e was a considerable challenge and the sequence was only carried out for the phenyl derivative. The isomers 6b–e displayed markedly reduced binding affinity to the DAT compared to 6a (Fig. 2).

The present work was part of a line of research conducted in our group intending to find new monoamine transport inhibitors preferably with selectivity between inhibition of DAT binding and uptake.<sup>25</sup> One medicinal chemistry strategy we wished to follow was simplification of the tropane skeleton and here the bicyclic compounds from the Trudell work became important as simpler analogues. We therefore decided to carry out an extended study of these compounds with many aromatic substituents. Since it has been reported that phenyltropanes (Fig. 3) having a 2,3-double bond (8a–c)<sup>11</sup> are equipotent with the saturated 2β,3β-substituted parents (7a–c) we chose to investigate the unsaturated derivatives thereby avoiding the problematic reduction of the double bond. The potency towards the SERT however was decreased dramatically, but since we were



**Scheme 1.** Reagents and conditions: (i)  $\text{AgNO}_3$ , NBS, acetone, rt, 2 h; (ii)  $95^\circ\text{C}$ , 24 h; (iii)  $\text{H}_2$ , 10% Pd/C, cyclohexane, rt, 12 h; (iv)  $\text{Ar-B(OH)}_2$ ,  $\text{Na}_2\text{CO}_3$ ,  $\text{Pd(OAc)}_2$ ,  $\text{PPh}_3$ , Benzene–EtOH,  $75^\circ\text{C}$ , 20 h; (v) TFA, DCM, rt, 20 h. X =  $-\text{CH}_2-$ ,  $-\text{O}-$ ,  $-\text{N(Boc)-}$ .

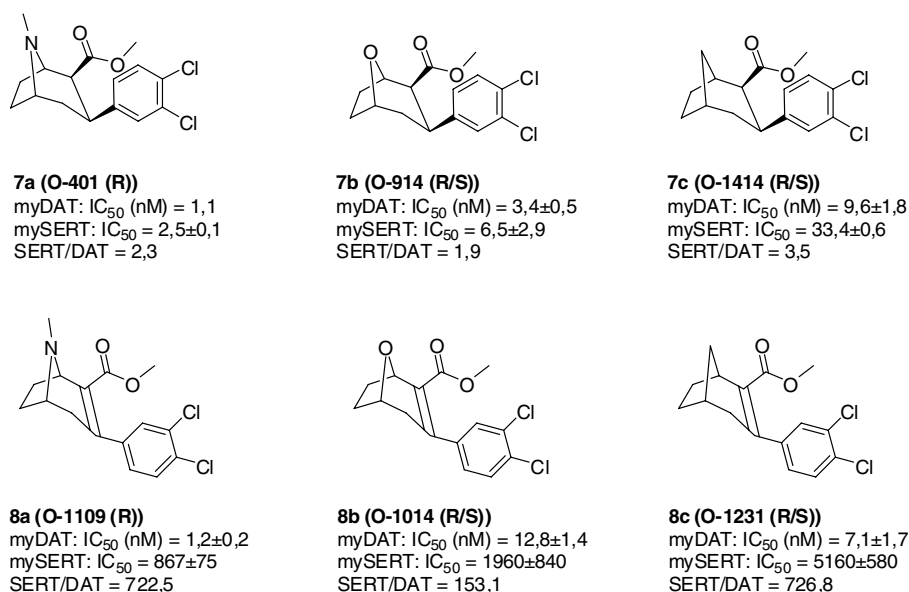


**Figure 3.** An example of a phenyl tropane and structural modifications hereof.

mainly concerned with DAT affinity this was no problem.

In the study we also addressed the structural simplification offered by deleting the nitrogen atom in the bridge-head position. In a very interesting recent study Meltzer and collaborators have shown that the nitrogen atom in the phenyl tropane (**7a**) is non-essential for binding. Oxa and carba analogues **7b** and **7c** were only 3- and 9-fold less potent than **7a** for binding to the DAT.<sup>22–24</sup> The synthetic scheme was therefore varied to include oxa and carba analogues of the 2:2:1-bicyclic compounds (Fig. 4).

The compounds **9<sub>x</sub>**–**11<sub>x</sub>**, **14**–**16**, **19**–**21** are derived from a truncated tropane skeleton which arises when removing C-4<sup>21</sup> (numbering from (–)-Cocaine (**1**)), while compounds **12<sub>x</sub>** and **17** arise from removing the bridge-head atom from these compounds, and finally compounds **13<sub>x</sub>** and **18** arise from removing C-5 and C-6 (numbering from **9**) from compounds **9<sub>x</sub>**. We herein describe the generation of 2D QSAR equations utilizing Cerius2<sup>19</sup> and furthermore we identify a pharmacophore by the methods implemented in Catalyst 4.10<sup>20</sup> both of which can relate molecular properties to the experimentally measured hDAT binding affinities of the compounds. We

reach the conclusion that the derived 2D QSAR equation is not as powerful as the 3D QSAR derived pharmacophore model with respect to predicting binding affinity of similar new next generation compounds.

## 2. Methods

### 2.1. Synthesis

All compounds with a bicyclic core-structure were prepared as outlined in Scheme 1. Compound **23** was obtained by bromination of **22** utilizing *N*-bromosuccinimide (NBS) and AgNO<sub>3</sub>, **23** was subsequently mixed with the cyclopentadiene **24** affording the Diels–Alder coupling product **25**. Upon hydrogenation of **25** with H<sub>2</sub> and Pd/C, **26** was produced, which was then subjected to a Suzuki coupling with the appropriate aromatic boronic acid to yield the desired coupling products. Compounds containing the *N*-Boc-group was finally subdued to a deprotection step with trifluoroacetic acid (TFA) resulting in the products outlined in Figure 4.

Compounds with a monocyclic core **12**–**13** and **17**–**18** were synthesized according to the reaction path outlined

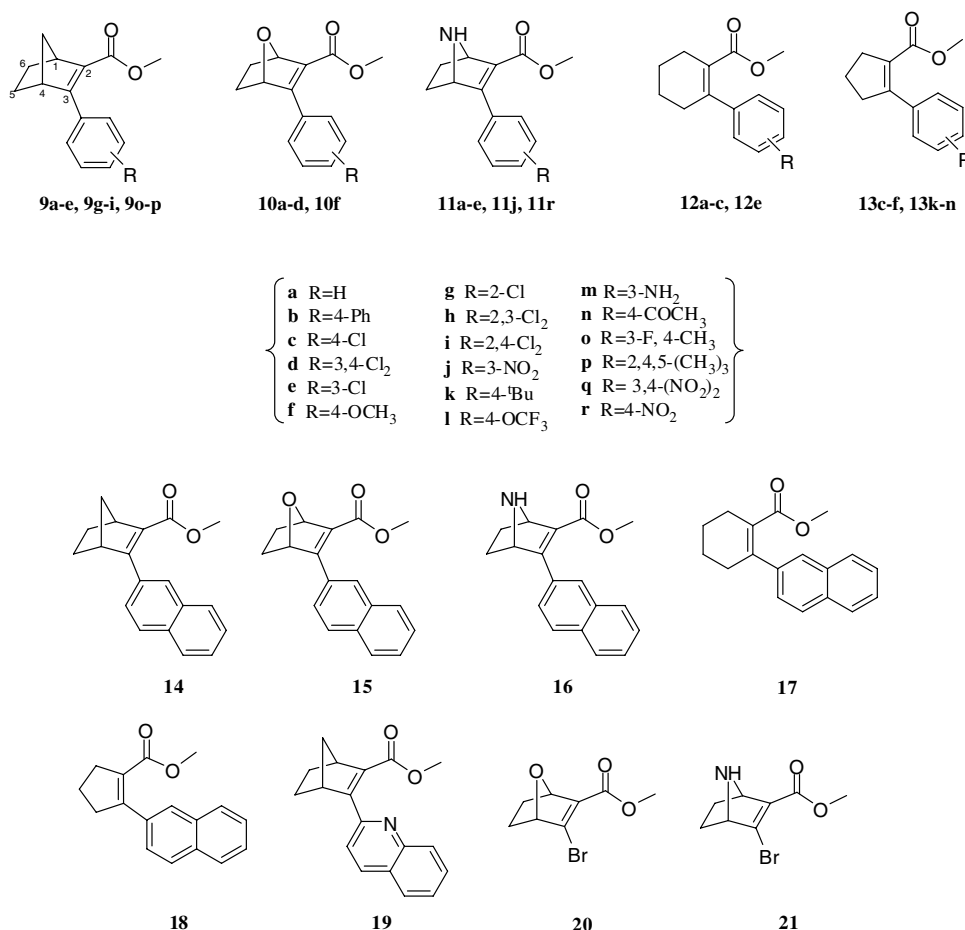
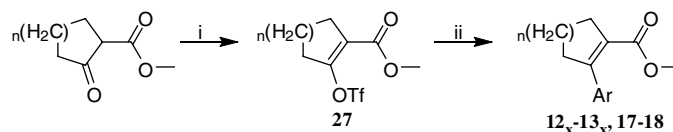


**Figure 4.** Chemical structures of the data set molecules. The notation letter after the compound number is used to refer to all the variants included in this figure for compounds **9<sub>x</sub>**–**13<sub>x</sub>**.



**Scheme 2.** Reagents and conditions: (i) NaH, TfO<sub>2</sub>, Et<sub>2</sub>O, rt, 1 h; (ii) Ar–B(OH)<sub>2</sub>, Na<sub>2</sub>CO<sub>3</sub>, Pd(OAc)<sub>2</sub>, PPh<sub>3</sub>, Benzene–EtOH, 75 °C, 20 h. *n* = 1,2.

in **Scheme 2**. Starting either from commercially available 2-oxo-cyclopentanecarboxylic acid methyl ester (*n* = 1) or 2-oxocyclohexanecarboxylic acid methyl ester (*n* = 2) and reacting it with NaH and Triflic anhydride (Tf<sub>2</sub>O) gave rise to the triflate-derivative **27**. Subsequent Suzuki-coupling with the appropriate boronic acids yielded the compounds **12–13** and **17–18**.

## 2.2. Biology

All compounds were tested for inhibition of the hDAT. This was carried out by determining displacement of a radioligand, according to the procedure described in Section 4.

## 2.3. Molecular modelling

QSAR modelling concerns the extraction of a quantitative relationship between the experimentally observed biological activity of a set of compounds and a number of descriptors related to physical and chemical properties of the compounds.<sup>25</sup> The 29 molecules in the 2D QSAR data set were divided into a training set of 25 compounds (2D-TS) and a test set with four molecules (2D-TEST)—see **Table 1**. A satisfactory 2D QSAR relation was generated by using the Genetic Partial Least Squares methodology (G/PLS) as implemented in the Cerius2 suite of programs.<sup>19</sup> The G/PLS methodology combines a Genetic Function Approximation (GFA)<sup>26</sup> for selecting the appropriate descriptors for the QSAR-model, and a Partial Least Squares (PLS)<sup>27</sup> regression as the fitting technique to weigh the relative contribution of each descriptor in the final model. The GFA method provides a population of QSAR-models rather than a single equation for correlation between biological activity and physicochemical descriptors. These models are created by evolving random initial models using a genetic algorithm. The next generation of models is computed by cross-over combinations between the best scoring models. PLS has proved superior in handling data with strongly correlated and numerous independent variables.<sup>28</sup> PLS, in particular, is able to identify linear combinations of the original physicochemical descriptors that are better for correlating the data thereby providing statistically more robust solutions.<sup>28</sup> Backtracking the final equation to the original variables is easy within PLS and provides a better way of chemical interpretation of the result. In this study, all descriptors within the Cerius2 QSAR+ module were included in the derivation of the QSAR equation, and the G/PLS methodology thus is appropriate in deriving robust QSAR relations consisting of a minimum number of descriptors.<sup>19</sup> Once derived, the equation was tested against the test set, 2D-TEST. Furthermore it was

**Table 1.** Actual and estimated pK<sub>i</sub> (–log(K<sub>i</sub>)) values using the 2D QSAR model

Compound	Actual –log(K <sub>i</sub> )	Estimated –log(K <sub>i</sub> )	Residual
2D-QSAR TS DAT binding			
<b>9a</b>	3.19	3.13	0.06
<b>9b</b>	3.22	3.98	–0.76
<b>9c</b>	4.60	4.16	0.44
<b>9d</b>	5.17	5.54	–0.37
<b>9g</b>	3.43	3.35	0.08
<b>9h</b>	4.83	4.76	0.07
<b>9i</b>	4.64	4.08	0.56
<b>11a</b>	3.35	3.92	–0.57
<b>11b</b>	4.61	4.28	0.33
<b>11c</b>	4.57	4.68	–0.11
<b>11d</b>	5.96	5.97	–0.01
<b>12a</b>	3.20	3.03	0.17
<b>12c</b>	4.07	3.87	0.20
<b>12e</b>	3.93	4.08	–0.15
<b>10c</b>	4.74	4.15	0.59
<b>13e</b>	4.46	4.68	–0.22
<b>13f</b>	3.85	3.82	0.03
<b>13k</b>	3.52	3.66	–0.14
<b>13l</b>	2.58	2.92	0.34
<b>13m</b>	3.06	2.89	0.17
<b>13n</b>	3.48	3.92	–0.44
<b>14</b>	5.37	5.35	0.02
<b>16</b>	5.76	5.73	0.03
<b>17</b>	4.93	4.83	0.10
<b>18</b>	5.38	5.14	0.24
2D QSAR TEST DAT binding			
<b>9e</b>	3.98	4.41	–0.43
<b>11e</b>	4.47	4.92	–0.45
<b>12b</b>	3.58	3.30	0.28
<b>13d</b>	5.71	5.29	0.42

checked by synthesizing and testing the biological activity of a set of analogues that were predicted to exhibit better pharmacological activity towards DAT.

The Catalyst 4.10 software package can be applied for automated ligand-based pharmacophore generation. Using the algorithm HypoGen<sup>29</sup> provided the quantitative 3D QSAR models for describing the binding affinity to hDAT. In this method an activity based alignment among a collection of conformations for each compound in the training set is obtained. The 3D pharmacophore models, called ‘hypotheses’, were derived from a data set containing 28 compounds of which 19 were used as the training set (3D-TS) and the remaining 9 served the test set (3D-TEST)—see **Table 2** for the details. The molecules were carefully chosen with respect to discrepancy in biological activity among a library consisting of a total of 42 compounds in the structural distinct sub-libraries (**9–21**).

**Table 2.** Actual and estimated  $pK_i$  values using the 3D QSAR model

Compound	Actual $K_i$	Estimated $K_i$	Error score
3D QSAR TS DAT binding			
<b>9a</b>	2.44	2.92	-3.1
<b>9h</b>	4.82	4.70	1.3
<b>10d</b>	5.12	5.51	-2.4
<b>11a</b>	3.35	2.64	5.2
<b>11d</b>	5.96	5.49	2.9
<b>11e</b>	4.47	4.39	1.2
<b>12a</b>	3.20	3.00	1.7
<b>12e</b>	4.67	4.68	-1.0
<b>13d</b>	5.71	5.92	-1.6
<b>13e</b>	4.46	4.48	-1.0
<b>13f</b>	3.85	4.68	-6.7
<b>13m</b>	3.06	3.08	-1.1
<b>14</b>	5.37	5.07	2.0
<b>16</b>	5.76	5.11	4.3
<b>17</b>	4.93	5.00	-1.1
<b>19</b>	4.48	4.80	-2.0
<b>20</b>	2.44	2.57	-1.4
<b>21</b>	2.39	2.64	-1.8
3D QSAR TES DAT binding			
<b>9b</b>	3.22	3.43	-1.6
<b>9d</b>	5.17	5.28	-1.3
<b>10c</b>	4.46	3.48	9.5
<b>10f</b>	3.24	4.22	-9.7
<b>11b</b>	4.60	3.39	17.0
<b>11c</b>	4.57	4.18	2.4
<b>12c</b>	4.07	4.41	-2.2
<b>13c</b>	4.74	4.55	1.5
<b>18</b>	5.38	4.81	3.3
3D QSAR prediction set DAT binding			
<b>9o</b>	4.25	4.74	-3.2
<b>9p</b>	4.49	4.47	1.0

### 3. Results and discussion

The best 2D QSAR model (highest  $q^2$ ) for hDAT binding calculated using G/PLS method found in Cerius2 resulted in Eq. (1).

$$-\log K_i = 4.00 - 3.93E_{\text{LUMO}} - 0.67E_{\text{HOMO}} - 3.24\sigma_p \quad (1)$$

$E_{\text{LUMO}}$  and  $E_{\text{HOMO}}$  are the energies of the LUMO and HOMO computed by CNDO/2, respectively, and  $\sigma_p$  is the Hammett constant of a substituent in the *para*-position. Having  $r^2 = 0.87$  and  $q^2 = 0.83$ , it is a case of a good model bordering to a perfect model. The predictive residual sum of squares (PRESS) is low (3.59) and comparing residual-values for the ligands in 2D-TES results in high residual-values, yet not higher than residual-values contained in the 2D-TS. Figure 5 depicts the plot of the actual activities versus the estimated activities (see

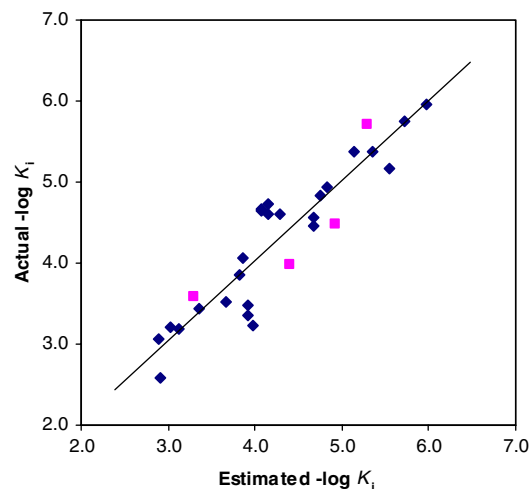
**Figure 5.** Plot of actual  $-\log K_i$  versus estimated  $-\log K_i$  of training set (◆) and test set (■) using 2D QSAR.  $R^2 = 0.8596$ .

Table 1 for actual numbers). The three descriptors that G/PLS found most valuable for assessing the binding to hDAT are all indicative of the importance of electronic effects of groups attached to the aromatic system. Better binding is predicted by a low  $E_{\text{LUMO}}$  energy (positive LUMO energies are computed), a large negative HOMO energy (negative HOMO energies are found) and a negative  $\sigma_p$ . Electron-withdrawing groups make the two former terms positive, while the Hammett constant term is negative and thus a moderating contribution.

As the model contains only three descriptors, it is relatively straightforward to suggest new potentially good ligands. By investigating different substituents at the phenyl-moiety, it became obvious that nitro-groups were predicted to have a very beneficial effect on the  $K_i$  value. Compound **11r** (with a *para*-nitro group) was predicted to have a  $K_i$  value of 1.5 nM, whilst the 3,4-disubstituted compound, **11q**, was predicted to have a  $K_i$  value of 0.3 pM. The 3,4-disubstituted compound, **11q**, was not synthesized though several unsuccessful attempts at synthesizing the equivalent boronic acid were performed. We therefore synthesized the mono-substituted nitro-compounds **11j** and **11r**, and subsequently tested them for biological activity giving the results shown in Table 3. Instead of having affinities in the low nanomolar range, these compounds give affinities in the high micromolar range, 232  $\mu\text{M}$  for **11j** and 68  $\mu\text{M}$  for **11r**. Clearly, introduction of the nitro-groups had an effect on binding affinity that was not described well by the derived 2D QSAR equation. Therefore, the

**Table 3.** Prediction of  $K_i$  values<sup>a</sup> (M) for the binding of nitro-substituted compounds to DAT with the 2D and 3D QSAR relations

Compound	Actual $K_i$	2D QSAR estimated $K_i$	Errorscore	3D QSAR estimated $K_i$	Errorscore
<b>11j</b>	$2.32 \cdot 10^{-4}$	$3.02 \cdot 10^{-11}$	-77,00,000	$4.1 \cdot 10^{-4}$	1.8
<b>11q</b>	n.a.	$5.89 \cdot 10^{-13}$	n.a.	$1.8 \cdot 10^{-3}$	n.a.
<b>11r</b>	$6.79 \cdot 10^{-5}$	$1.51 \cdot 10^{-9}$	-45,000	$3.8 \cdot 10^{-3}$	56

<sup>a</sup> All values specified in M. n.a., not available. Errorscore =  $-\text{Act.}K_i/\text{Est.}K_i$  if Est. < Act.; =  $\text{Act.}K_i/\text{Est.}K_i$  if Est. > Act.

investigation was extended to include a 3D QSAR study applying the Catalyst software to see whether this tool could provide a better model. On the basis of manually selected compounds, features and settings, this program can design 3D models that not only suggest generalized three dimensional orientations of chemical features, but also estimate the biological activities of the compounds in the training and test sets.

Using Catalyst's HypoGen module, and selecting from a set of 52 structurally diverse ligands that vary in activity values over about 3 orders of magnitude, a 3D QSAR model was obtained. The quality of the generated pharmacophore hypothesis was evaluated from the cost functions calculated by HypoGen during hypothesis generation.<sup>29</sup> The structures of the molecules used are found in Figure 5 and all biological activities are shown in Table 2. The result of the hypothesis generation can be seen in Table 4 where the 10 generated hypotheses are summarized.

Figure 6 depicts the plot of the actual activities versus the estimated activities obtained with Hypo1 (the estimated activities are tabulated in Table 2). The top scoring hypothesis, Hypo1, with one hydrogen bond acceptor, two hydrophobes, one aliphatic hydrophobe and one aromatic hydrophobe features displays a fixed cost of 72.245, total cost of 78.123 and null cost of 117.69 with a configuration cost of 7.209 bits, all of which are acceptable values indicating a good fit. The difference between the fixed and the null cost has to be 20–80 bits, and in this case the difference was 45.45, which is reasonable. The difference in cost between total and null of 39.568 indicates a 70–80% statistical significance bordering the 80–90%, the consequence of this is that there is approximately 80% chance of obtaining a predictive hypothesis. This hypothesis also shows the lowest RMS (0.787) and the highest correlation coefficient (0.944) and thus Hypo1 was retained for further analysis. The test set was estimated with errorscores ranging from –9.7 (10f) to 17 (11b), but most errorscores are in the acceptable range of –4 to 4 (Table 2).

To validate Hypo1's ability of prediction, we prepared the two compounds, **9o** and **9p**, the activities of which had been predicted by Hypo1 to be in the  $\mu\text{M}$  range.

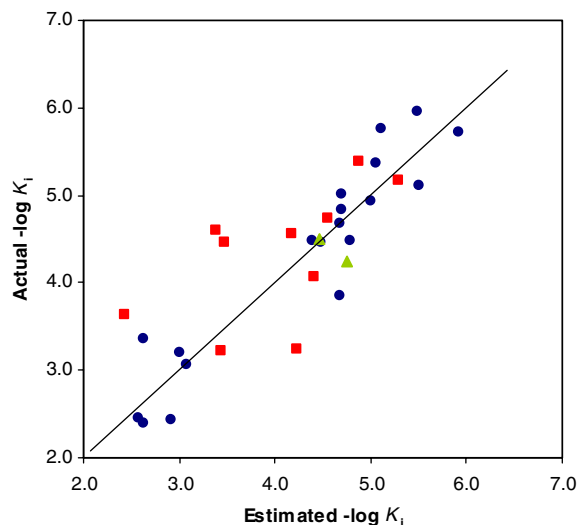


Figure 6. Plot of actual  $-\log K_i$  versus estimated  $-\log K_i$  of training set (●), test set (■) and prediction set (▲) using 3D QSAR.  $R^2 = 0.8907$ .

Table 5. Prediction set and  $K_i$  values<sup>a</sup> for DAT predicted by top ranking Hypo1

Compound	Actual $K_i$	Estimated $K_i$	Errorscore
<b>9o</b>	$5.60 \cdot 10^{-5}$	$1.8 \cdot 10^{-5}$	–3.2
<b>9p</b>	$3.22 \cdot 10^{-5}$	$3.4 \cdot 10^{-5}$	1.0

<sup>a</sup> All values specified in M. Errorscore:  $-\text{Act./Est.}$

As can be seen from Table 5, Hypo1 demonstrated a high degree of predictability for these two ligands with errorscores in the low range (1.0 and –3.2). Figure 7 depicts **9p** fitted in Hypo1 using the flexible fit option.

With this piece of evidence at hand, we turned to the more difficult problem of predicting the activity of the two nitro-substituted compounds (Table 3). While, Hypo1 could not predict the  $K_i$  values of nitro-substituted compounds perfectly it nevertheless predicted them considerably better than the 2D QSAR model was able to do. This can also intuitively be rationalized when visualizing the graphic model (Fig. 7), since it possesses two hydrophobic moieties in the position where

Table 4. Summary of the HypoGen output for the 3D-TS data set

Hypo <sup>a</sup>	Total cost	Cost difference <sup>b</sup>	RMS	Correlation ( $r$ )	Features <sup>c</sup>
Hypo1	78.123	39.568	0.787	0.944	HBA, HY, HYAl, HYAr, HY
Hypo2	78.400	39.290	0.801	0.942	HBA, HY, HYAl, HY, HY
Hypo3	78.527	39.163	0.805	0.941	HBA, HY, HYAr, HY, HY
Hypo4	78.824	38.866	0.831	0.937	HBA, HY, HY, HY, HY
Hypo5	79.372	38.318	0.864	0.932	HBA, HY, HYAl, HY, RAr
Hypo6	79.731	37.959	0.883	0.929	HBA, HY, HY, HY, RAr
Hypo7	81.955	35.735	1.010	0.905	HBA, HY, HYAl, HY, RAr
Hypo8	84.055	33.636	1.094	0.888	HBA, HY, HY, HY, RAr
Hypo9	84.094	33.596	1.111	0.885	HBA, HY, HYAl, HYAl, RAr
Hypo10	84.722	32.969	1.129	0.881	HBA, HY, HY, HY, RAr

<sup>a</sup> Numbers for the hypotheses are consistent with the numeration as obtained by the hypothesis generation.

<sup>b</sup> Difference between the null hypothesis and the total cost of each returned hypothesis.

<sup>c</sup> HBA: hydrogen bond acceptor; HY: Hydrophobic; HYAl: aliphatic hydrophobe; HYAr: aromatic hydrophobe; RAr: ring aromatic.

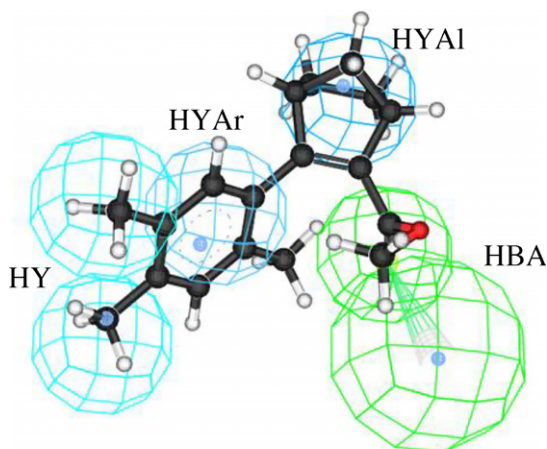


**Figure 7.** The top scoring Hypo1 is mapped to compound **9p**. HBA: hydrogen bond acceptor, HY: hydrophobe, HYAl: aliphatic hydrophobe, and HYAr: aromatic hydrophobe.

the nitro-groups are. The nitro-group is polar and therefore, based on the 3D pharmacophore model, these compounds are predicted and actually overestimated to a poor affinity. In any case it is obvious that the nitro derivatives are difficult to predict with models that are based on training sets not containing nitro-substituted compounds.

It is interesting to compare the two new models with existing QSAR models of related compounds. Comparison with the models made for phenyltropanes<sup>15,30</sup> is particularly relevant since the compounds in this study are truncated versions of phenyltropanes and are likely to have a similar binding at the ester and aromatic region. Carroll et al. have reported a 2D QSAR model for para substituted phenyl tropanes that has the equation  $\text{pIC}_{50} = 0.46\pi + 0.20MR - 0.01MR^2 - 1.51$  meaning that lipophilicity and size are the important factors for the substituent in the aromat.<sup>30</sup> This is in contrast to our 2D model which exclusively correlates the activity to electronic effects, which reflects that the binding of the aromatic group, in the two classes of compounds, is not identical. It is observed that, even though both classes of compounds show similar trends (i.e., chloro-substitution increases potency, etc.), the influence of substitution is much larger for the small non-nitrogen containing compounds. It is possible that these smaller compounds, which do not interact at the nitrogen binding site, can enter deeper into an aromatic binding pocket thereby obtaining stronger and possibly different interactions.

3D QSAR models, in the form of CoMFA, have also been reported on phenyl tropanes<sup>15,31</sup> and on structurally related benzotropines.<sup>17</sup> These models indicate that small to medium size steric groups are favourable on the aromatic moiety while electronic effects are of less importance. The Hypo1 model points to reach a very similar conclusion since it points to hydrophilic groups attached to the aromatic group as being important for the binding. Thus 3D QSAR models of phenyl tropanes and the non-nitrogen containing analogues are qualitatively consistent.

### 3.1. Conclusions and perspectives

2D and 3D QSAR models were developed to describe the affinity for hDAT of the library of previously prepared compounds. Both models show that the aromatic moiety is very important. The 2D QSAR model is the relatively simple relationship  $\text{pK}_i = 4.00 - 3.93E_{\text{LUMO}} - 0.67E_{\text{HOMO}} - 3.24\sigma_p$ , which purely depends on electronic effects and which predicts that electron-withdrawing groups are favourable. In contrast, the 3D model predicts a number of hydrophobic areas around the aromatic moiety and it is therefore better in predicting the affinities of the nitro-substituted compounds than the 2D model. The models complement each other and appear to be useful predictive devices for further compound design.

## 4. Experimental

### 4.1. General

NMR spectra were recorded on a Varian Gemini 2000 Spectrometer (400 MHz concerning <sup>1</sup>H and 100 MHz concerning <sup>13</sup>C) with tetramethylsilane (TMS) as the internal standard and CDCl<sub>3</sub> as the solvent and reference point ( $\delta$  7.26 ppm and  $\delta$  77.16 ppm, respectively). Mass spectra were recorded at a Micromass LC-TOF spectrometer. Thin layer chromatography (TLC) was carried out on silica gel (Merck Kieselgel 60 F<sub>254</sub>) and for visualization of the spots either UV light (254 nm) or Ce-Mol solution (Ce(SO<sub>4</sub>)<sub>2</sub> (10 g) and (NH<sub>4</sub>)<sub>2</sub>MoO<sub>4</sub> (15 g) dissolved in 10% H<sub>2</sub>SO<sub>4</sub>) was applied. Flash column chromatography was carried out on Merck silica gel (230–400 mesh). Reactions were conducted under an atmosphere of nitrogen.

### 4.2. Preparation of Suzuki coupling derivatives. General synthetic procedure

1 Equiv methyl 3-bromo-bicyclo[2.2.1]hept-2-ene-2-carboxylate (**26**) was added to a 5 mL vial with PPh<sub>3</sub> (0.1 equiv), Na<sub>2</sub>CO<sub>3</sub> (2 equiv), Pd(OAc)<sub>2</sub> (0.05 equiv) and dissolved in ethanol–benzene (1/3, 4 mL). Finally, the boronic acid (1.2 equiv) was added, and the resulting mixture flushed with nitrogen. While stirring, the mixture was heated to 75 °C for 20 h.

**4.2.1. Methyl 3-phenyl-bicyclo[2.2.1]hept-2-ene-2-carboxylate (9a).** Purification by flash chromatography (diethyl ether–pentane; 1/30) afforded **9a** as colourless oil in 99% yield (226 mg, 0.99 mmol). <sup>1</sup>H NMR (CDCl<sub>3</sub>)  $\delta$  7.53 (m, 2H), 7.33 (m, 3H), 3.67 (s, 3H), 3.39 (br s, 1H), 3.28 (br s, 1H), 1.89 (m, 2H), 1.66 (ddd, 1H,  $J_1 = 2.0$  Hz,  $J_2 = 3.8$  Hz,  $J_3 = 8.5$  Hz), 1.39 (m, 2H), 1.25 (d, 1H,  $J = 8.5$  Hz); <sup>13</sup>C NMR (CDCl<sub>3</sub>)  $\delta$  166.0, 158.0, 135.3, 132.2, 128.4, 128.3, 127.7, 51.1, 50.2, 46.7, 45.4, 26.1, 25.8; HR-MS (ES) calcd for C<sub>15</sub>H<sub>16</sub>O<sub>2</sub> + Na<sup>+</sup>:  $m/z$  251.1048. Found  $m/z$  251.1044.

**4.2.2. Methyl 3-(4-biphenyl)-bicyclo[2.2.1]hept-2-ene-2-carboxylate (9b).** Purification by flash chromatography (diethyl ether–pentane; 1/30) afforded **9b** as colourless

oil in 94% yield (69 mg, 0.23 mmol).  $^1\text{H}$  NMR ( $\text{CDCl}_3$ )  $\delta$  7.67 (d, 2H,  $J = 7.8$  Hz), 7.63 (d, 2H,  $J = 7.8$  Hz), 7.60 (d, 2H,  $J = 7.8$  Hz), 7.46 (t, 2H,  $J = 7.6$  Hz), 7.36 (t, 1H,  $J = 7.4$  Hz), 3.72 (s, 3H), 3.44 (br s, 1H), 3.34 (br s, 1H), 1.93 (m, 2H), 1.70 (m, 1H), 1.43 (dd, 2H,  $J_1 = 2.0$  Hz,  $J_2 = 7.3$  Hz), 1.29 (d, 1H,  $J = 8.6$  Hz);  $^{13}\text{C}$  NMR ( $\text{CDCl}_3$ )  $\delta$  166.0, 157.7, 141.0, 140.7, 134.0, 132.5, 128.9, 128.7, 127.4, 127.0, 126.4, 51.1, 50.1, 46.5, 45.5, 26.2, 25.7; HR-MS (ES) calcd for  $\text{C}_{19}\text{H}_{18}\text{O}_2 + \text{Na}^+$ :  $m/z$  327.1361. Found  $m/z$  327.1358.

**4.2.3. Methyl 3-(4-chlorophenyl)-bicyclo[2.2.1]hept-2-ene-2-carboxylate (9c).** Purification by flash chromatography (diethyl ether–pentane; 1/30) afforded **9c** as colourless oil in 70% yield (40 mg, 0.15 mmol).  $^1\text{H}$  NMR ( $\text{CDCl}_3$ )  $\delta$  7.48 (d, 2H,  $J = 8.8$  Hz), 7.30 (d, 2H,  $J = 8.8$  Hz), 3.68 (s, 3H), 3.38 (br s, 1H), 3.23 (br s, 1H), 1.89 (m, 2H), 1.65 (d, 1H,  $J = 8.8$  Hz), 1.36 (m, 2H), 1.25 (d, 1H,  $J = 8.8$  Hz);  $^{13}\text{C}$  NMR ( $\text{CDCl}_3$ )  $\delta$  165.8, 156.8, 134.1, 133.6, 133.1, 129.8, 127.9, 51.2, 50.1, 46.7, 45.4, 26.1, 25.7; HR-MS (ES) calcd for  $\text{C}_{15}\text{H}_{15}\text{ClO}_2 + \text{Na}^+$ :  $m/z$  285.0658. Found  $m/z$  285.0667.

**4.2.4. Methyl 3-(3,4-dichlorophenyl)-bicyclo[2.2.1]hept-2-ene-2-carboxylate (9d).** Purification by flash chromatography (diethyl ether–pentane; 1/30) afforded **9d** as colourless oil in 93% yield (88 mg, 0.30 mmol).  $^1\text{H}$  NMR ( $\text{CDCl}_3$ )  $\delta$  7.64 (s, 1H), 7.39 (s, 2H), 3.69 (s, 3H), 3.40 (br s, 1H), 3.22 (br s, 1H), 1.91 (m, 2H), 1.64 (ddd, 1H,  $J_1 = 1.9$  Hz,  $J_2 = 4.0$  Hz,  $J_3 = 8.5$  Hz), 1.36 (m, 2H), 1.26 (d, 1H,  $J = 8.5$  Hz);  $^{13}\text{C}$  NMR ( $\text{CDCl}_3$ )  $\delta$  165.5, 155.3, 135.2, 134.3, 132.1, 131.9, 130.2, 129.7, 127.9, 51.3, 50.0, 46.7, 45.5, 26.0, 25.7; HR-MS (ES) calcd for  $\text{C}_{15}\text{H}_{14}\text{Cl}_2\text{O}_2 + \text{Na}^+$ :  $m/z$  319.0269. Found  $m/z$  319.0268.

**4.2.5. Methyl 3-(3-chlorophenyl)-bicyclo[2.2.1]hept-2-ene-2-carboxylate (9e).** Purification by flash chromatography (diethyl ether–pentane; 1/30) afforded **9e** as colourless oil in 87% yield (50 mg, 0.19 mmol).  $^1\text{H}$  NMR ( $\text{CDCl}_3$ )  $\delta$  7.50 (br s, 1H), 7.40 (m, 1H), 7.27 (m, 2H), 3.68 (s, 3H), 3.39 (br s, 1H), 3.23 (br s, 1H), 1.90 (m, 2H), 1.65 (d, 1H,  $J = 8.8$  Hz), 1.36 (m, 2H), 1.25 (d, 1H,  $J = 8.8$  Hz);  $^{13}\text{C}$  NMR ( $\text{CDCl}_3$ )  $\delta$  165.6, 156.8, 137.1, 133.8, 133.7, 129.0, 128.3, 128.2, 126.6, 51.2, 50.1, 46.8, 45.5, 26.0, 25.7; HR-MS (ES) calcd for  $\text{C}_{15}\text{H}_{15}\text{ClO}_2 + \text{Na}^+$ :  $m/z$  285.0658. Found  $m/z$  285.0649.

**4.2.6. Methyl 3-(2-chlorophenyl)-bicyclo[2.2.1]hept-2-ene-2-carboxylate (9g).** Purification by flash chromatography (diethyl ether–pentane; 1/30) afforded **9g** as colourless oil in 50% yield (32 mg, 0.12 mmol).  $^1\text{H}$  NMR ( $\text{CDCl}_3$ )  $\delta$  7.39 (m, 1H), 7.22 (m, 2H), 7.08 (m, 1H), 3.58 (s, 3H), 3.40 (br s, 1H), 3.21 (br s, 1H), 1.83 (m, 3H), 1.35 (m, 3H);  $^{13}\text{C}$  NMR ( $\text{CDCl}_3$ )  $\delta$  165.3, 155.9, 135.9, 135.5, 132.7, 129.5, 129.4, 128.9, 126.2, 51.1, 50.5, 47.3, 44.2, 25.7, 24.6; HR-MS (ES) calcd for  $\text{C}_{15}\text{H}_{15}\text{ClO}_2 + \text{Na}^+$ :  $m/z$  285.0658. Found  $m/z$  285.0659.

**4.2.7. Methyl 3-(2,3-dichlorophenyl)-bicyclo[2.2.1]hept-2-ene-2-carboxylate (9h).** Purification by flash chromatography (diethyl ether–pentane; 1/30) afforded **9h** as colourless oil in 59% yield (49 mg, 0.16 mmol).  $^1\text{H}$

NMR ( $\text{CDCl}_3$ )  $\delta$  7.40 (d, 1H,  $J = 8.1$  Hz), 7.15 (t, 1H,  $J = 7.8$  Hz), 6.95 (d, 1H,  $J = 7.6$  Hz), 3.58 (s, 3H), 3.40 (br s, 1H), 3.19 (br s, 1H), 1.85 (m, 3H), 1.35 (m, 3H);  $^{13}\text{C}$  NMR ( $\text{CDCl}_3$ )  $\delta$  165.0, 155.6, 137.7, 136.2, 133.1, 131.0, 129.6, 127.5, 126.8, 51.2, 50.4, 47.4, 44.1, 25.7, 24.6; HR-MS (ES) calcd for  $\text{C}_{15}\text{H}_{14}\text{Cl}_2\text{O}_2 + \text{Na}^+$ :  $m/z$  319.0269. Found  $m/z$  319.0259.

**4.2.8. Methyl 3-(2,4-dichlorophenyl)-bicyclo[2.2.1]hept-2-ene-2-carboxylate (9i).** Purification by flash chromatography (diethyl ether–pentane; 1/30) afforded **9i** as colourless oil in 65% yield (50 mg, 0.17 mmol).  $^1\text{H}$  NMR ( $\text{CDCl}_3$ )  $\delta$  7.41 (d, 1H,  $J = 2.2$  Hz), 7.20 (dd, 1H,  $J_1 = 2.2$  Hz,  $J_2 = 8.3$  Hz), 7.02 (d, 1H,  $J = 8.3$  Hz), 3.59 (s, 3H), 3.40 (br s, 1H), 3.18 (br s, 1H), 1.85 (m, 3H), 1.32 (m, 3H);  $^{13}\text{C}$  NMR ( $\text{CDCl}_3$ )  $\delta$  165.1, 154.8, 136.6, 134.0, 133.5, 130.3, 129.3, 126.6, 51.2, 50.4, 47.4, 44.2, 25.6, 24.6; HR-MS (ES) calcd for  $\text{C}_{15}\text{H}_{14}\text{Cl}_2\text{O}_2 + \text{Na}^+$ :  $m/z$  319.0269. Found  $m/z$  319.0262.

**4.2.9. Methyl 3-(3-fluoro-4-methyl-phenyl)-bicyclo[2.2.1]hept-2-ene-2-carboxylate (9o).** Prepared by employing the Suzuki coupling procedure described above affording a colourless oil in 95% yield after purification by flash chromatography (diethyl ether–pentane; 1/25).  $^1\text{H}$  NMR:  $\delta$  7.25–7.23 (m, 1H), 7.22 (s, 1H), 7.13 (t, 1H), 3.68 (s, 3H), 3.37–3.36 (m, 1H), 3.24–3.23 (m, 1H), 2.27 (d, 3H), 1.92–1.86 (m, 2H), 1.64 (dt, 1H), 1.35 (tt, 2H), 1.24 (dt, 1H);  $^{13}\text{C}$  NMR:  $\delta$  166.0, 159.6, 156.8, 134.7, 133.0, 130.7, 125.1, 124.1, 115.1, 51.3, 50.2, 46.7, 45.7, 26.3, 25.8, 14.6; HR-MS (ES) calcd for  $\text{C}_{16}\text{H}_{17}\text{FO}_2 + \text{Na}^+$ : 283.1110. Found: 283.1118.

**4.2.10. Methyl 3-(2,4,5-trimethyl-phenyl)-bicyclo[2.2.1]hept-2-ene-2-carboxylate (9p).** Prepared by employing the Suzuki coupling procedure described above affording a colourless oil in 58% yield after purification by flash chromatography (diethyl ether–pentane; 1/25).  $^1\text{H}$  NMR:  $\delta$  6.98 (s, 1H), 6.76 (s, 1H), 3.58 (s, 3H), 3.38–3.37 (m, 1H), 3.08–3.06 (m, 1H), 2.22 (s, 3H), 2.20 (s, 3H), 2.16 (s, 3H), 1.88–1.79 (m, 2H), 1.72 (dt, 1H), 1.41–1.32 (m, 2H), 1.25 (dt, 1H);  $^{13}\text{C}$  NMR:  $\delta$  165.9, 159.5, 136.1, 134.4, 133.7, 133.3, 132.9, 131.5, 128.7, 51.2, 51.1, 47.2, 44.4, 26.0, 24.9, 19.6, 19.4, 19.3; HR-MS (ES) calcd for  $\text{C}_{18}\text{H}_{22}\text{O}_2 + \text{Na}^+$ : 293.1517. Found: 293.1517.

**4.2.11. Methyl 3-phenyl-7-oxabicyclo[2.2.1]hept-2-ene-2-carboxylate (10a).** Purification by flash chromatography (diethyl ether–pentane; 1/30) afforded **10a** as colourless crystals (mp 89.5–90.0 °C) in 93% yield (107 mg, 0.46 mmol).  $^1\text{H}$  NMR ( $\text{CDCl}_3$ )  $\delta$  7.67 (d, 2H,  $J = 6.7$  Hz), 7.38 (m, 3H), 5.35 (d, 1H,  $J = 3.0$  Hz), 5.31 (d, 1H,  $J = 3.8$  Hz), 3.74 (s, 3H), 2.03 (m, 2H), 1.53 (m, 2H);  $^{13}\text{C}$  NMR ( $\text{CDCl}_3$ )  $\delta$  164.2, 155.8, 131.8, 131.3, 129.4, 128.6, 128.2, 83.1, 81.0, 51.5, 25.5, 25.0; HR-MS (ES) calcd for  $\text{C}_{14}\text{H}_{14}\text{O}_3 + \text{Na}^+$ :  $m/z$  253.0841. Found  $m/z$  253.0838.

**4.2.12. Methyl 3-(4-chlorophenyl)-7-oxabicyclo[2.2.1]hept-2-ene-2-carboxylate (10c).** The reaction mixture was filtered and the solvents were evaporated under reduced pressure. Flash chromatography (pentane/EtOAc 10:1)

afforded **10c** in 79% yield (42 mg, 0.16 mmol).  $^1\text{H}$  NMR ( $\text{CDCl}_3$ )  $\delta$  7.63 (d, 2H,  $J = 8.6$  Hz), 7.35 (d, 2H,  $J = 8.6$  Hz), 5.34 (d, 1H,  $J = 3.4$  Hz), 5.27 (d, 1H,  $J = 3.7$  Hz), 3.75 (s, 3H), 2.02 (m, 2H), 1.51 (m, 2H);  $^{13}\text{C}$  NMR ( $\text{CDCl}_3$ )  $\delta$  163.8, 154.4, 135.3, 132.2, 129.5, 129.8, 128.3, 82.7, 80.8, 51.4, 25.2, 24.8; HR-MS (ES) calcd for  $\text{C}_{18}\text{H}_{16}\text{O}_3 + \text{Na}^+$ :  $m/z$  287.0451. Found  $m/z$  287.0450.

**4.2.13. Methyl 3-(3,4-dichlorophenyl)-7-oxabicyclo[2.2.1]hept-2-ene-2-carboxylate (10d).** The reaction mixture was filtered through Celite and purified by flash chromatography (pentane/EtOAc 10:1) to yield the product, **10d**, as brown/yellowish oil (34 mg, 11 mmol, 56%).  $^1\text{H}$  NMR ( $\text{CDCl}_3$ )  $\delta$  7.80 (d, 1H,  $J = 2.1$  Hz), 7.53 (d, 1H,  $J = 2.1$  Hz), 7.46 (s, 1H), 5.34 (dd, 1H,  $J_1 = 1.1$  Hz,  $J_2 = 4.3$  Hz), 5.26 (dd, 1H,  $J_1 = 1.0$  Hz,  $J_2 = 4.6$  Hz), 3.76 (s, 3H), 2.04 (m, 2H), 1.54 (m, 2H);  $^{13}\text{C}$  NMR ( $\text{CDCl}_3$ )  $\delta$  162.8, 152.3, 143.2, 139.8, 132.5, 132.2, 129.4, 129.2, 127.0, 81.6, 80.1, 50.7, 24.3, 24.0.

**4.2.14. Methyl 3-(4-methoxy-phenyl)-7-oxabicyclo[2.2.1]hept-2-ene-2-carboxylate (10f).** Prepared by employing the Suzuki coupling procedure described above affording a yellow oil in 53% yield after purification by flash chromatography (EtOAc–pentane; 1/5).  $^1\text{H}$  NMR:  $\delta$  7.67 (d, 2H); 6.89 (d, 2H) 5.30 (m, 2H); 3.81 (s, 3H); 3.73 (s, 3H); 1.89 (m, 2H); 1.46 (m, 2H).

**4.2.15. Methyl 3-phenyl-7-azabicyclo[2.2.1]hept-2-ene-2-carboxylate (11a).** Crude Boc-protected **11a**, a yellowish oil (320 mg, 0.97 mmol), was dissolved in 10 mL DCM and reacted with 2 mL TFA (26 mmol) for 20 h which resulted in removal of the Boc-group. Purification by flash chromatography (1/15, MeOH–DCM) yielded **11a** as a yellowish oil in 95% yield (211 mg, 0.92 mmol).  $^1\text{H}$  NMR ( $\text{CDCl}_3$ )  $\delta$  7.59 (m, 2H), 7.36 (m, 3H), 4.77 (br s, 1H), 4.76 (br s, 1H), 3.71 (s, 3H), 2.20 (m, 2H), 1.51 (m, 2H);  $^{13}\text{C}$  NMR ( $\text{CDCl}_3$ )  $\delta$  163.7, 155.0, 130.9, 129.8, 128.7, 128.2, 65.7, 62.9, 51.7, 24.1, 23.4; HR-MS (ES) calcd for  $\text{C}_{14}\text{H}_{15}\text{NO}_2 + \text{H}^+$ :  $m/z$  230.1181. Found  $m/z$  230.1016.

**4.2.16. Methyl 3-(4-biphenyl)-7-tert-butoxycarbonyl-7-azabicyclo[2.2.1]hept-2-ene-2-carboxylate (Boc-11b).** The reaction mixture was filtered through Celite and purified by flash chromatography (pentane/EtOAc 10:1) to yield the product, **Boc-11b**, as a colourless solid (mp 92–95 °C) (71 mg, 0.18 mmol, 87%).  $^1\text{H}$  NMR ( $\text{CDCl}_3$ )  $\delta$  7.72 (d, 2H,  $J = 8.5$  Hz), 7.62 (m, 4H), 7.45 (t, 2H,  $J = 7.2$  Hz), 7.37 (t, 1H,  $J = 7.2$  Hz), 5.09 (s, 1H), 5.06 (s, 1H), 3.76 (s, 3H), 2.11 (m, 2H), 1.53 (m, 2H), 1.44 (s, 9H);  $^{13}\text{C}$  NMR ( $\text{CDCl}_3$ )  $\delta$  164.6, 155.2, 142.4, 140.6, 131.1, 129.9, 129.8, 129.5, 129.1, 127.3, 127.1, 127.9, 80.7, 65.8, 63.2, 51.8, 28.5, 28.3, 28.2; HR-MS (ES) calcd for  $\text{C}_{25}\text{H}_{27}\text{NO}_4 + \text{Na}^+$ :  $m/z$  428.1840. Found  $m/z$  428.1831.

**4.2.17. Methyl 3-(4-biphenyl)-7-azabicyclo[2.2.1]hept-2-ene-2-carboxylate (11b).** **Boc-11b** (71 mg, 0.18 mmol) was dissolved in 10 mL DCM and reacted with 2 mL TFA (26 mmol) for 20 h which resulted in removal of the Boc-group. The solvent and TFA were evaporated

under reduced pressure and flash chromatography in DCM/MeOH 10:1 afforded **11b** as a yellow/brown oil in 99% yield.  $^1\text{H}$  NMR ( $\text{CDCl}_3$ )  $\delta$  7.72 (d, 2H,  $J = 8.4$  Hz), 7.59 (d, 4H,  $J = 8.5$  Hz), 7.42 (t, 2H,  $J = 7.4$  Hz), 7.34 (t, 1H,  $J = 7.4$  Hz), 4.55 (d, 1H,  $J = 1.6$  Hz), 4.52 (d, 1H,  $J = 2.3$  Hz), 3.73 (s, 3H), 2.06 (m, 2H), 1.44 (m, 2H);  $^{13}\text{C}$  NMR ( $\text{CDCl}_3$ )  $\delta$  165.2, 158.3, 141.6, 140.2, 134.7, 131.5, 128.8, 128.7, 126.9, 126.6, 127.5, 66.4, 63.5, 51.2, 25.4, 25.0; HR-MS (ES) calcd for  $\text{C}_{20}\text{H}_{19}\text{NO}_2 + \text{H}^+$ :  $m/z$  306.1494. Found  $m/z$  306.1494.

**4.2.18. Methyl 3-(4-chlorophenyl)-7-tert-butoxycarbonyl-7-azabicyclo[2.2.1]hept-2-ene-2-carboxylate (Boc-11c).** The reaction mixture was filtered through Celite and purified by flash chromatography (pentane/EtOAc 10:1) to yield the product, **Boc-11c**, as colourless oil (65 mg, 0.18 mmol, 89%).  $^1\text{H}$  NMR ( $\text{CDCl}_3$ )  $\delta$  7.56 (d, 2H,  $J = 8.1$  Hz), 7.35 (d, 2H,  $J = 8.1$  Hz), 5.06 (s, 1H), 5.00 (s, 1H), 3.74 (s, 3H), 2.09 (m, 2H), 1.49 (m, 2H), 1.45 (s, 9H);  $^{13}\text{C}$  NMR ( $\text{CDCl}_3$ )  $\delta = 163.5$ , 154.5, 154.4, 134.9, 129.9, 129.6, 127.9, 80.1, 65.0, 62.4, 51.1, 27.7, 25.2, 25.1; HR-MS (ES) calcd for  $\text{C}_{19}\text{H}_{22}\text{NO}_4\text{Cl} + \text{Na}^+$ :  $m/z$  386.1135. Found  $m/z$  386.1137.

**4.2.19. Methyl 3-(4-chlorophenyl)-7-azabicyclo[2.2.1]hept-2-ene-2-carboxylate (11c).** **Boc-11c** (65 mg, 0.18 mmol) was dissolved in 10 mL DCM and reacted with 2 mL TFA (26 mmol) for 20 h which resulted in removal of the Boc-group. The solvent and TFA were evaporated under reduced pressure and flash chromatography in DCM/MeOH 10:1 afforded **11c** as a colourless oil in 99% yield.  $^1\text{H}$  NMR ( $\text{CDCl}_3$ )  $\delta$  7.59 (d, 2H,  $J = 8.5$  Hz), 7.33 (d, 2H,  $J = 8.5$  Hz), 4.55 (d, 1H,  $J = 2.6$  Hz), 4.45 (d, 1H,  $J = 2.9$  Hz), 3.73 (s, 3H), 2.04 (m, 2H), 1.43 (m, 2H);  $^{13}\text{C}$  NMR ( $\text{CDCl}_3$ )  $\delta = 164.9$ , 157.3, 135.2, 134.8, 131.0, 129.6, 128.2, 66.3, 63.5, 51.3, 25.3, 24.9; HR-MS (ES) calcd for  $\text{C}_{14}\text{H}_{14}\text{NO}_2\text{Cl} + \text{H}^+$ :  $m/z$  264.0791. Found  $m/z$  264.0785.

**4.2.20. Methyl 3-(3,4-dichlorophenyl)-7-*N*-tert-butyl-7-azabicyclo[2.2.1]hept-2-ene-2-carboxylate (Boc-11d).** The reaction mixture was filtered through Celite and purified by flash chromatography (pentane/EtOAc 10:1) to yield the product, **Boc-11d**, as brown/yellowish oil in 97% (77 mg, 0.19 mmol).  $^1\text{H}$  NMR ( $\text{CDCl}_3$ )  $\delta$  7.91 (s, 1H), 7.64 (s, 1H), 7.45 (s, 1H), 5.25 (s, 1H), 5.13 (s, 1H), 3.94 (s, 3H), 2.30 (m, 2H), 1.63 (m, 2H), 1.61 (s, 9H).

**4.2.21. Methyl 3-(3,4-dichlorophenyl)-7-azabicyclo[2.2.1]hept-2-ene-2-carboxylate (11d).** **Boc-11d** (77 mg, 0.19 mmol) was dissolved in 10 mL DCM and reacted with 2 mL TFA (26 mmol) for 20 h, which resulted in removal of the Boc-group. The solvent and TFA were evaporated under reduced pressure and flash chromatography in DCM/MeOH 15:2 afforded **11d** as a colourless oil in 97% yield.  $^1\text{H}$  NMR ( $\text{CDCl}_3$ )  $\delta$  7.75 (s, 1H), 7.50 (d, 1H,  $J = 8.4$  Hz), 7.43 (d, 1H,  $J = 8.4$  Hz), 4.56 (m, 1H), 4.44 (m, 1H), 3.74 (s, 3H), 2.03 (m, 2H), 1.41 (m, 2H);  $^{13}\text{C}$  NMR ( $\text{CDCl}_3$ )  $\delta$  164.6, 155.8, 136.2, 132.6, 132.4, 132.0, 129.8, 129.7, 127.4, 66.0,

63.4, 51.3, 25.1, 24.8; HR-MS (ES) calcd for  $C_{14}H_{13}NO_2Cl_2 + H^+$ :  $m/z$  298.0402. Found  $m/z$  298.0396.

**4.2.22. Methyl 3-(3-chlorophenyl)-7-*N*-tert-butoxycarbonyl-7-azabicyclo[2.2.1]hept-2-ene-2-carboxylate (Boc-11e).** The reaction mixture was filtered through Celite and purified by flash chromatography (pentane/EtOAc; 10:1) to yield the product, **Boc-11e**, as brown/yellowish oil in 91% (66 mg, 0.18 mmol).  $^1H$  NMR ( $CDCl_3$ )  $\delta$  7.59 (s, 1H), 7.48 (d, 1H,  $J = 6.9$  Hz), 7.32 (m, 2H), 5.06 (s, 1H), 5.00 (s, 1H), 3.74 (s, 3H), 2.09 (m, 2H), 1.48 (m, 2H), 1.43 (s, 9H);  $^{13}C$  NMR ( $CDCl_3$ )  $\delta$  163.9, 155.0, 154.9, 134.1, 133.8, 129.4, 129.3, 128.6, 126.8, 80.6, 65.6, 62.9, 51.6, 28.2, 25.5, 25.1; HR-MS (ES) calcd for  $C_{19}H_{22}NO_4Cl + Na^+$ :  $m/z$  386.1135. Found  $m/z$  386.1136.

**4.2.23. Methyl 3-(3-chlorophenyl)-7-azabicyclo[2.2.1]hept-2-ene-2-carboxylate (11e).** **Boc-11e** (66 mg, 0.18 mmol) was dissolved in 10 mL DCM and reacted with 2 mL TFA (26 mmol) for 20 h, which resulted in removal of the Boc-group. The solvent and TFA were evaporated under reduced pressure and flash chromatography in DCM/MeOH 15:2 afforded **11e** as a colourless oil in 99% yield.  $^1H$  NMR ( $CDCl_3$ )  $\delta$  7.62 (s, 1H), 7.52 (m, 1H), 7.31 (m, 2H), 4.58 (d, 1H,  $J = 3.4$  Hz), 4.49 (d, 1H,  $J = 3.8$  Hz), 3.74 (s, 3H), 2.07 (m, 2H), 1.44 (m, 2H); HR-MS (ES) calcd for  $C_{14}H_{14}NO_2Cl + H^+$ :  $m/z$  264.0791. Found  $m/z$  264.0793.

**4.2.24. Methyl 3-(3-nitro-phenyl)-7-azabicyclo[2.2.1]hept-2-ene-2-carboxylate (11j).** Prepared by employing the Suzuki coupling procedure described above affording a colourless oil in 97% yield after purification by flash chromatography (MeOH–DCM; 1/12).  $^1H$  NMR:  $\delta$  8.46 (s, 1H); 8.20 (d, 1H); 7.94 (d, 1H); 7.56 (t, 1H); 4.79 (s, 1H); 4.78 (s, 1H); 3.75 (s, 3H); 2.23 (m, 2H); 1.57 (m, 2H).  $^{13}C$  NMR:  $\delta$  162.9, 152.7, 147.7, 134.2, 129.0, 123.8, 123.2, 133.9, 132.7, 65.3, 62.6, 51.7, 23.8, 23.5. HR-MS (ES) calcd for  $C_{14}H_{14}N_2O_4 + H^+$ :  $m/z$  275.1032. Found: 275.1027.

**4.2.25. Methyl 3-(4-nitro-phenyl)-7-azabicyclo[2.2.1]hept-2-ene-2-carboxylate (11r).** Prepared by employing the Suzuki coupling procedure described above affording a colourless oil in 97% yield after purification by flash chromatography (MeOH–DCM; 1/12)  $^1H$  NMR:  $\delta$  8.20 (d, 2H) 7.77 (d, 2H); 4.60 (d, 1H); 4.48 (d, 1H); 3.73 (s, 3H); 2.07 (m, 2H); 1.46 (m, 2H).  $^{13}C$  NMR:  $\delta$  164.6, 156.3, 147.5, 139.6, 129.9, 129.1, 128.3, 123.2, 66.6, 63.8, 51.7, 25.2. HR-MS (ES) calcd for  $C_{14}H_{14}N_2O_4 + H^+$ :  $m/z$  275.1032. Found: 275.1040.

**4.2.26. Methyl 2-(3-aminophenyl)cyclopent-1-enecarboxylate (12m).** Purification by flash chromatography (diethyl ether–pentane; 1/1) afforded **9m** as yellowish oil in 86% yield (30 mg, 0.14 mmol).  $^1H$  NMR ( $CDCl_3$ )  $\delta$  7.11 (t, 1H,  $J = 7.8$  Hz); 6.70 (d, 1H,  $J = 7.6$  Hz); 6.65 (s, 1H); 6.62 (d, 1H,  $J = 7.9$  Hz); 3.63 (s, 3H); 2.81 (t, 4H,  $J = 7.7$  Hz +  $H_{a+b}^5$ ); 1.97 (p, 2H,  $J = 7.7$  Hz).  $^{13}C$  NMR ( $CDCl_3$ )  $\delta$  166.8; 153.5; 145.9; 138.0; 128.7; 118.1; 114.8; 114.3; 51.1; 40.1; 35.1; 21.9. HR-MS (ES) calcd for  $C_{13}H_{15}NO_2 + H^+$ :  $m/z$  218.1181. Found: 218.1179.

**4.2.27. Methyl 2-(4-acetylphenyl)cyclopent-1-enecarboxylate (12n).** Purification by flash chromatography (diethyl ether–pentane; 1/1) afforded **9n** as colourless oil in 79% yield (50 mg, 0.20 mmol).  $^1H$  NMR ( $CDCl_3$ )  $\delta$  7.92 (d, 2H,  $J = 8.5$  Hz); 7.39 (d, 2H,  $J = 8.5$  Hz); 3.62 (s, 3H); 2.85 (m, 4H); 2.59 (s, 3H); 2.01 (p, 2H,  $J = 7.7$  Hz).  $^{13}C$  NMR ( $CDCl_3$ )  $\delta$  197.6; 166.1; 152.5; 142.0; 136.2; 130.5; 127.9, 127.8; 51.3; 40.0; 35.1; 26.6; 22.0. HR-MS (ES) calcd for  $C_{15}H_{16}O_3 + Na^+$ :  $m/z$  267.0997. Found: 267.1000.

**4.2.28. Methyl 3-(2-naphthyl)-bicyclo[2.2.1]hept-2-ene-2-carboxylate (14).** Purification by flash chromatography (diethyl ether–pentane; 1/30) afforded **14** as colourless oil in 63% yield (42 mg, 0.15 mmol).  $^1H$  NMR ( $CDCl_3$ )  $\delta$  8.00 (s, 1H), 7.83 (m, 2H), 7.79 (d, 1H,  $J = 8.4$  Hz), 7.63 (d, 1H,  $J = 8.4$  Hz), 7.47 (m, 2H), 3.68 (s, 3H), 3.44 (br s, 1H), 3.40 (br s, 1H), 1.95 (m, 2H), 1.74 (d, 1H,  $J = 8.8$  Hz), 1.45 (m, 2H), 1.30 (d, 1H,  $J = 8.8$  Hz);  $^{13}C$  NMR ( $CDCl_3$ )  $\delta$  166.0, 158.0, 133.1, 132.9\*2, 132.8, 128.3, 127.5\*2, 127.1, 126.5, 126.3, 126.1, 51.1, 50.3, 46.7, 45.5, 26.2, 25.8; HR-MS (ES) calcd for  $C_{19}H_{18}O_2 + Na^+$ :  $m/z$  301.1204. Found  $m/z$  301.1205.

**4.2.29. Methyl 3-(2-naphthyl)-7-oxabicyclo[2.2.1]hept-2-ene-2-carboxylate (15).** The reaction mixture was filtered through Celite and purified by flash chromatography (pentane–EtOAc 10/1) to yield the product, **15**, as a yellow solid (38 mg, 0.14 mmol, 68%).  $^1H$  NMR ( $CDCl_3$ )  $\delta$  8.13 (s, 1H), 7.83 (m, 4H), 7.50 (m, 2H), 5.44 (d, 2H,  $J = 4.6$  Hz), 5.41 (d, 2H,  $J = 4.2$  Hz), 3.76 (s, 3H), 2.06 (m, 2H), 1.59 (m, 2H).  $^{13}C$  NMR ( $CDCl_3$ )  $\delta$  164.3, 155.8, 133.6, 132.9, 132.1, 28.8, 128.6, 128.4, 127.8, 127.6, 127.1, 126.4, 126.1, 83.2, 81.2, 51.5, 25.6, 25.2; HR-MS (ES) calcd for  $C_{18}H_{16}O_3 + Na^+$ :  $m/z$  303.0997. Found  $m/z$  303.0999.

**4.2.30. Methyl 3-(2-naphthyl)-7-tert-butoxycarbonyl-7-azabicyclo[2.2.1]hept-2-ene-2-dicarboxylate (Boc-16).** The reaction mixture was filtered through Celite and purified by flash chromatography (pentane–EtOAc, 10/1) to yield the product, **Boc-16**, as brown/yellowish oil in 90% (68 mg, 0.18 mmol).  $^1H$  NMR ( $CDCl_3$ )  $\delta$  8.09 (s, 1H), 7.87 (m, 2H), 7.83 (d, 1H,  $J = 8.4$  Hz), 7.69 (d, 1H,  $J = 8.4$  Hz), 7.50 (m, 2H), 5.12 (s, 2H), 3.75 (s, 3H), 2.13 (m, 2H), 1.57 (m, 2H), 1.45 (s, 9H);  $^{13}C$  NMR ( $CDCl_3$ )  $\delta$  164.1, 154.9, 142.2, 133.3, 132.6, 128.2, 128.3, 127.4\*2, 126.8, 126.2, 126.0, 80.3, 62.8, 58.7, 51.3, 28.0, 27.9\*2; HR-MS (ES) calcd for  $C_{23}H_{25}NO_4 + Na^+$ :  $m/z$  402.1681. Found  $m/z$  402.1678.

### 4.3. Binding assays

1. *Cell cultures.*<sup>8</sup> Cell lines stably expressing hDAT were established by transfecting COS-1 cells with hDAT inserted in the pIRES vector (BD Biosciences Clontech) also carrying a Blastocidin resistance gene. Cells were cultured in DMEM (BioWhittaker) supplemented with 10% FCS (Gibco Life Technologies), 1% penicillin/streptomycin (BioWhittaker) and 10  $\mu$ g/mL of Blastocidin (Cayla) selection of transfected cells. After 14 days of selection, blastocidin was

adjusted to 2 µg/mL in the culture medium and the cells were subcultured under this selection regime and grown at 37 °C, 5% CO<sub>2</sub> and 95% humidity.

2. **Binding assay.**<sup>8</sup> Membrane preparations for the binding assay were produced by scraping the stably transfected cells from cell culture dishes (Nunc), pelleting the cells in ice-cold PBSCM by centrifugation and homogenizing the cells in ice-cold harvest buffer I (150 mM NaCl, 50 mM Tris, 20 mM EDTA) using an Ultra-Turrax (Janke and Kunkel AG) for 60 s. The membrane was pelleted by centrifugation at 12000g for 10 min at 4 °C and washed in ice-cold Harvest buffer I. The membranes were pelleted again and, finally, resuspended in PBSCM using Ultraturax briefly. Membrane preparations were aliquoted into 2 mL portions and stored at –80 °C until use. The concentration of total protein in the membrane preparation was determined with the MicroBCA kit (Pierce). A concentration of 5 µg/well of membrane preparation was used with the chosen concentration of drug of interest in combination with 0.1–0.25 nM <sup>125</sup>I-RTI-55. Membrane and ligands were incubated for 1 h at 20 °C using a Filtermate cell harvester (Packard), membranes were captured on GF/B 96-well filterplates (Packard) presoaked with 0.5% polyethyleneimine (Merck) and washed thrice with ice-cold water. The filter in each well was dissolved in 40 µL Microscint 20 and scintillation counts were determined with a Packard Topcounter. Precise concentration of radioligand was quantified by liquid scintillation counting on a Packard Tri-Carb.
3. **Data analysis.** Counts from the Packard Topcounter were fitted to a sigmoidal dose–response curve using the built-in nonlinear regression tool in the Graphpad Prism 3 software. From at least three independent experiments, the resulting IC<sub>50</sub> values were transformed into K<sub>i</sub> values using the equation described by Cheng and Prusoff.<sup>32</sup>

## 5. Molecular modelling

### 5.1. General

Calculations were performed on a Silicon Graphics Octane2 R12000 workstation running under the IRIX 6.5.12 operating system. QSAR relations were computed using either Cerius2 or Catalyst software packages.<sup>19,20</sup> Initial drawing and minimization of the compounds were done in Cerius2 or Catalyst.

### 5.2. 2D QSAR

The biological activities were entered manually. The 2D QSAR equations were generated using the G/PLS method in Cerius2. A population of 100 randomly constructed equations was initially built by use of the default settings and the built-in descriptors. These equations were then evolved for 50,000 generations (default 5000). Evolving the equations means that, for each generation, two better scoring equations are selected as parents. Parts of each parent equation are then combined into a child equation. Only better scoring child equa-

tions will be included in the parent population and substitute for the worst of the parents. This will leave the best 100 equations for the next evolution. The scoring of the equations was validated by calculating the predictive residual sum of squares (PRESS) and through the cross-validation test implemented in Cerius2.<sup>19</sup> The highest  $q^2$  and the lowest difference between  $q^2$  and  $r^2$  were used to select the best equation. Furthermore, the ability of the best equation to predict binding of compounds in the test set was assessed.

### 5.3. 3D QSAR

Minimized structures of the compounds were imported into Catalyst. Compounds not containing conformational information were drawn and minimized in Catalyst and subsequently subjected to a conformational search using ‘Best’ conformational generation, as recommended when utilizing the HypoGen module. The training set was chosen from the libraries with respect to activities, so that the most active and the least active along with some intermediate actives from each library were chosen for the HypoGen generation. The biological data were entered manually. All parameter values were left to default, and the features were chosen to be hydrogen-bond acceptor, hydrophobe, hydrophobe aliphatic, hydrophobic aromatic and ring aromatic. Each hypothesis was set to contain a minimum of 5 and a maximum of 10 features. The generated models were evaluated in terms of cost analysis, and the capability of predicting activities was evaluated with a test set and a prediction set.

### Acknowledgments

We are indebted to Steffen Sinning and Ove Wiborg for performing the biological tests. We also thank the Lundbeck Foundation, the Carlsberg Foundation and FNU for financial support.

### Supplementary data

Supporting information contains carbon-13 NMR spectra of compounds **9o**, **9p**, **10f**, **11j**, **11r**, **12m** and **12n** (8 pages), and the results of catscramble analysis of hypo 1. Supplementary data associated with this article can be found, in the online version, at [doi:10.1016/j.bmc.2007.05.015](https://doi.org/10.1016/j.bmc.2007.05.015).

### References and notes

1. Carroll, F. I.; Howell, L. L.; Kuhar, M. J. *Med. Chem.* **1999**, *42*, 2721–2736.
2. Singh, S. *Chem. Rev.* **2000**, *100*, 925–1024.
3. Kuhar, M. J.; Ritz, M. C.; Boja, J. W. *Trends Neurosci.* **1991**, *14*, 299–302.
4. Carroll, F. I. *J. Med. Chem.* **2003**, *46*, 1775–1794.
5. Pedersen, H.; Sinning, S.; Bülow, A.; Wiborg, O.; Falborg, L.; Bols, M. *Org. Biomol. Chem.* **2004**, *2*, 2861–2869.
6. Iso, Y.; Grajkowska, E.; Wroblewski, J. T.; Davis, J.; Goeders, N. E.; Johnson, K. M.; Sanker, S.; Roth, B. L.;

- Tueckmantel, W.; Kozikowski, A. P. *J. Med. Chem.* **2006**, *49*, 1080–1100.
7. Carroll, F. I.; Lewin, A. H.; Boja, J. W.; Kuhar, M. J. *J. Med. Chem.* **1992**, *35*, 969–981.
  8. Bülow, A.; Sinning, S.; Wiborg, O.; Bols, M. *J. Comb. Chem.* **2004**, *6*, 509–519.
  9. Newman, A. H.; Allen, A. C.; Izenwasser, S.; Katz, J. L. *J. Med. Chem.* **1994**, *37*, 2258–2261.
  10. Kozikowski, A. P.; Araldi, G. L.; Boja, J. W.; Meil, W. M.; Johnson, K. M.; Flippen-Anderson, J. L.; George, C.; Saiah, E. *J. Med. Chem.* **1998**, *41*, 1962–1969.
  11. Tamiz, A. P.; Zhang, J.; Flippen-Anderson, J. L.; Zhang, M.; Johnson, K. M.; Deschaux, O.; Tella, S.; Kozikowski, A. P. *J. Med. Chem.* **2000**, *43*, 1215–1222.
  12. Enyedy, I. J.; Zaman, W. A.; Sakamuri, S.; Kozikowski, A. P.; Johnson, K. M.; Wang, S. *Bioorg. Med. Chem. Lett.* **2001**, *11*, 1113–1118.
  13. Meltzer, P. C.; Butler, D.; Deschamps, J. R.; Madras, B. K. *J. Med. Chem.* **2006**, *49*, 1420–1432.
  14. Crammer, R. D.; Patterson, D. E.; Bunce, J. D. *J. Am. Chem. Soc.* **1988**, *110*, 5959–5967.
  15. Carroll, F. I.; Gao, Y. G.; Rahman, M. A.; Abraham, P.; Parham, K.; Lewin, A. H.; Boja, J. W.; Kuhar, M. J. *J. Med. Chem.* **1991**, *34*, 2719–2725.
  16. Newman, A. H.; Izenwasser, S.; Robarge, M. J.; Kline, R. H. *J. Med. Chem.* **1999**, *42*, 3502–3509.
  17. Kulkarni, S. S.; Grundt, P.; Kopajtic, T.; Katz, J. L.; Newman, A. H. *J. Med. Chem.* **2004**, *47*, 3388–3398.
  18. Yuan, H.; Kozikowski, A. P.; Petukhov, P. A. *J. Med. Chem.* **2004**, *47*, 6137–6143.
  19. Cerius<sup>2</sup> version 4.9, Accelrys: San Diego, USA, 2004.
  20. Catalyst version 4.10, Accelrys: San Diego, USA, 2005.
  21. Zhang, C.; Izenwasser, S.; Katz, J. L.; Terry, P. D.; Trudell, M. L. *J. Med. Chem.* **1998**, *41*, 2430–2435.
  22. Meltzer, P. C.; Liang, A. Y.; Blundell, P.; Gonzalez, M. D.; Chen, Z.; George, C.; Madras, B. K. *J. Med. Chem.* **1997**, *40*, 2661–2673.
  23. Meltzer, P. C.; Blundell, P.; Young, Y. F.; Chen, Z.; George, C.; Gonzalez, M. D.; Madras, B. K. *J. Med. Chem.* **2000**, *43*, 2982–2991.
  24. Goulet, M.; Miller, G. M.; Bendor, J.; Liu, S.; Meltzer, P. C.; Madras, B. K. *Synapse* **2001**, 129–140.
  25. Petersen, M. D.; Boye, S. V.; Nielsen, E. H.; Sinning, S.; Wiborg, O.; Bols, M. *Bioorg. Med. Chem.* **2007**, *15*, 4159–4174.
  26. Fan, Y.; Shi, L. M.; Kohn, K. W.; Pommier, Y.; Weinstein, J. N. *J. Med. Chem.* **2001**, *44*, 3254–3263.
  27. Rogers, D.; Hopfinger, A. J. *J. Chem. Inf. Comput. Sci.* **1994**, *34*, 854–866.
  28. Glen, W. G.; Dunn, W. J., III; Scott, D. R. *Tetrahedron Comput. Meth.* **1989**, *2*, 349–376.
  29. Wold, S. In *Chemometric Methods in Molecular Design*; Van der Waterbeemd, H., Ed.; VCH Weinheim, 1995; pp 195–218.
  30. Li, H.; Sutter, J.; Hoffmann, R. HypoGen: an automated system for generating 3D predictive pharmacophore models. In: *Pharmacophore Perception, Development, and Use in Drug Design*; International University: La Jolla, CA, 2000, pp 171–189.
  31. Carroll, F. I.; Mascarella, S. W.; Kuzemko, M. A.; Gao, Y.; Abraham, P.; Lewin, A. H.; Boja, J. W.; Kuhar, M. J. *J. Med. Chem.* **1994**, *37*, 2865–2873.
  32. Cheng, Y.; Prusoff, W. H. *Biochem. Pharmacol.* **1973**, *22*, 3099–3108.